

Surface Corrections to the High-Energy Optical Potential*

R. E. SCHENTER AND B. W. DOWNS
University of Colorado, Boulder, Colorado
 (Received 27 September 1962)

The dependence of the nucleon-nucleon scattering matrix on the momentum transfer q is taken into account in a derivation of the high-energy (local) optical potential. This leads to an optical potential characterized by radial functions which have larger mean radii and more diffuse surfaces than does the nucleon distribution in the target nucleus, to which these functions reduce when the q dependence is neglected.

I. INTRODUCTION

THE elastic scattering of high-energy nucleons by nuclei can be described in terms of a local optical potential.^{1,2} In the usual form of this potential

$$V(\mathbf{r}) = V_c(r) + r^{-1}[dV_{so}(r)/dr]\boldsymbol{\sigma} \cdot \mathbf{L}, \quad (1)$$

the central and spin-orbit potential functions $V_c(r)$ and $V_{so}(r)$ are complex, and are frequently taken to have the same radial dependence.^{1,2}

Attempts to derive a local optical potential in terms of nucleon-nucleon interactions for the small-angle scattering of high-energy nucleons by medium and heavy nuclei have led to a potential of the form (1).^{1,2} In these derivations, the dependence of the nucleon-nucleon scattering matrix on the momentum transfer q is usually neglected³; the coefficients in this matrix (evaluated at $q=0$) then appear as factors in the potential functions $V_c(r)$ and $V_{so}(r)$. With the neglect of the q dependence, the radial dependence of the potential functions becomes that of the nucleon density $\rho(r)$ of the target nucleus.

Phenomenological analyses of high-energy elastic scattering data have led to specification of parameters which characterize the radial dependence of the potential functions in (1).^{1,2} The radial dependences thus deduced differ from those of the appropriate nucleon density functions in that they have larger mean radii and more diffuse surfaces.²

In Sec. II of this paper, account is taken of the q dependence of the nucleon-nucleon scattering matrix in a derivation of the local, high-energy optical potential. The radial dependence of the resulting optical potential has been calculated for targets with assumed nucleon densities representative of heavy nuclei. The results, which are given in Sec. III and discussed in Sec. IV, are found to improve the agreement between the derived and phenomenological optical potentials.

* Supported in part by a grant from the National Science Foundation.

¹ See, for example, H. Feshbach, *Ann. Rev. Nucl. Sci.* **8**, 49 (1958).

² See, for example, A. E. Glassgold, *Progr. Nucl. Phys.* **7**, 123 (1959).

³ Some account of the q dependence has been taken by A. K. Kerman, H. McManus, and R. M. Thaler, *Ann. Phys. (N.Y.)* **8**, 551 (1959), A. H. Cromer, *Phys. Rev.* **113**, 1607 (1959), and R. R. Johnson, *Nucl. Phys.* **36**, 368 (1962). Cromer, in particular, has emphasized the importance of the q dependence.

II. RADIAL DEPENDENCE OF THE OPTICAL POTENTIAL

The local form of the optical potential for elastic scattering, derived on the basis of the multiple scattering formalism of Watson⁴ or the high-energy approximation of Glauber,⁵ can be written as⁶

$$V(\mathbf{r}) = \frac{-2\hbar^2(N-1)}{(2\pi)^2 m} \int F(\mathbf{q}) \bar{M}(\mathbf{k}, \mathbf{k}') e^{i\mathbf{q} \cdot \mathbf{r}} d\mathbf{q}, \quad (2)$$

where $\bar{M}(\mathbf{k}, \mathbf{k}')$ is the nucleon-nucleon scattering matrix in the two-nucleon center-of-mass system averaged over spin and isotopic spin of the target nucleons, \mathbf{k} and \mathbf{k}' ($k'=k$) being the initial and final relative momentum vectors; N is the number of target nucleons, and m is the nucleon mass. The nuclear form factor

$$F(\mathbf{q}) = \int e^{-i\mathbf{q} \cdot \mathbf{r}} \rho(\mathbf{r}) d\mathbf{r}, \quad (3)$$

which is a function of the momentum transfer $\mathbf{q} = \mathbf{k}' - \mathbf{k}$, is the Fourier transform of the nucleon density function $\rho(\mathbf{r})$ (normalized to unity) of the target nucleus.

The most general form of the charge-symmetric nucleon-nucleon scattering matrix $M(\mathbf{k}, \mathbf{k}')$, which is invariant under space rotations, space reflections, and time reversal, is^{7,8}

$$M = A + B\sigma_n(1)\sigma_n(2) + C[\sigma_n(1) + \sigma_n(2)] \\ + E\sigma_q(1)\sigma_q(2) + F\sigma_p(1)\sigma_p(2), \quad (4)$$

where $\boldsymbol{\sigma}(1)$ and $\boldsymbol{\sigma}(2)$ are the Pauli spin operators for the incident and target nucleons, respectively; and $\sigma_n(1)$ is the component of $\boldsymbol{\sigma}(1)$ in the \hat{n} direction, etc. The unit vectors $\hat{n} = (\mathbf{k} \times \mathbf{k}') / |\mathbf{k} \times \mathbf{k}'|$, $\hat{q} = (\mathbf{k}' - \mathbf{k}) / |\mathbf{k}' - \mathbf{k}|$, and $\hat{p} = \hat{q} \times \hat{n}$ form an orthogonal set. The coefficients $A \cdots F$ depend upon the spin, isotopic spin, scattering angles, and energy in the nucleon-nucleon center-of-mass system.

⁴ W. B. Riesenfeld and K. M. Watson, *Phys. Rev.* **102**, 1157 (1956).

⁵ R. J. Glauber, in *Lectures in Theoretical Physics*, edited by W. E. Brittin and L. G. Dunham (Interscience Publishers, Inc., New York, 1959), Vol. I, p. 315.

⁶ A. K. Kerman, H. McManus and R. M. Thaler, *Ann. Phys. (N.Y.)* **8**, 551 (1959).

⁷ L. Wolfenstein and J. Ashkin, *Phys. Rev.* **85**, 947 (1952); L. Wolfenstein, *Ann. Rev. Nucl. Sci.* **6**, 43 (1956).

⁸ R. H. Dalitz, *Proc. Phys. Soc. (London)* **A65**, 175 (1952).

The scattering matrix $\bar{M}(\mathbf{k}, \mathbf{k}')$, which appears in (2), is the average of (4) over the spins of the target nucleons and over the isotopic spin states formed by the incident and target nucleons. The spins of most of the protons and neutrons being separately paired in nuclei, the averaging of the scattering matrix (4) over the spins of the target nucleons eliminates all terms containing $\sigma(2)$ up to order $1/N$.⁹ Then the averaging over isotopic spin states leads to a specification of the remaining coefficients in $\bar{M}(\mathbf{k}, \mathbf{k}')$. To order $1/N$, the result is^{6,10}

$$\bar{M}(\mathbf{k}, \mathbf{k}') = \bar{A}(k, q) + \bar{C}(k, q) \boldsymbol{\sigma} \cdot \hat{n} \quad (5)$$

with

$$\bar{A} = [(3A_1 + A_0) \pm (A_0 - A_1)(N_N - N_P)/N]/4, \quad (6a)$$

$$\bar{C} = [(3C_1 + C_0) \pm (C_0 - C_1)(N_N - N_P)/N]/4. \quad (6b)$$

The subscripts 1 and 0 in (6) are the values of the total isotopic spin in the nucleon-nucleon system; in the second terms, which are proportional to the neutron excess, the plus and minus signs apply to an incident proton and an incident neutron, respectively. The spin operator in (5) is that for the incident nucleon, the designation 1 having been dropped.

With the average scattering matrix (5) and the assumption that the target nucleon distribution $\rho(\mathbf{r})$ is spherically symmetric, (2) leads to an optical potential of the form (1) with^{4,6}

$$V_C(\mathbf{r}) = \frac{-2\hbar^2(N-1)}{(2\pi)^2 m} \int F(q) \bar{A}(k, q) e^{i\mathbf{q} \cdot \mathbf{r}} d\mathbf{q} \quad (7a)$$

and

$$V_{SO}(\mathbf{r}) = \frac{2i\hbar^2(N-1)}{(2\pi)^2 m} \int F(q) \bar{C}(k, q) (k^2 \sin\theta)^{-1} e^{i\mathbf{q} \cdot \mathbf{r}} d\mathbf{q}, \quad (7b)$$

where θ is the scattering angle in the nucleon-nucleon center-of-mass system [that is, $q = 2k \sin(\theta/2)$]. The average scattering matrix coefficients in (7) can be expressed as^{11,12}

$$\bar{A}(k, q) = \sum_l a_l(k) P_l(\mu) \quad (8a)$$

and

$$\bar{C}(k, q) (k^2 \sin\theta)^{-1} = \sum_l [c_l(k)/k^2] dP_l(\mu)/d\mu, \quad (8b)$$

where the expansion coefficients $a_l(k)$ and $c_l(k)$ are functions of the energy-dependent (spin) singlet and triplet nucleon-nucleon phase shifts corresponding to orbital angular momentum l .¹³ Equations (8) can be

⁹ When all spins in the target are paired, the form (5) is exact. The calculations reported in Sec. III of this paper were made for heavy nuclei for which $1/N$ is less than 0.01.

¹⁰ F. E. Bjorklund, B. A. Lippmann, and M. J. Moravcsik, Nucl. Phys. **29**, 582 (1962).

¹¹ H. P. Stapp, T. J. Ypsilantis, and N. Metropolis, Phys. Rev. **105**, 302 (1957).

¹² H. A. Bethe, Ann. Phys. (N. Y.) **3**, 190 (1958).

¹³ Explicit expressions for the expansion coefficients $a_l(k)$ and $c_l(k)$ in terms of nucleon-nucleon phase shifts can be obtained readily from references 6, 11, and 12. Expressions of the form (8) for the scattering matrix coefficients appearing in (6) are given in reference 12 [Eqs. (2.5) and (2.6) and the paragraph preceding Eqs. (2.9)]. The coefficients of the expansions in reference 12

expressed explicitly in terms of the momentum transfer q with the relation $\mu = \cos\theta = 1 - q^2/2k^2$ for the argument of the Legendre polynomials.

The essential steps in the development of this section are taken at this point: The relation

$$q^2 e^{i\mathbf{q} \cdot \mathbf{r}} = -\nabla^2 e^{i\mathbf{q} \cdot \mathbf{r}} \quad (9)$$

is used to replace the q^{2n} , which appear in the factors (8) in the potential functions (7), by the operators ∇^{2n} ; the factors (8) are then pulled out of the integrals in (7) with the results

$$V_C(\mathbf{r}) = \frac{-4\pi\hbar^2(N-1)}{m} \times \left[\sum_l a_l(k) P_l(\mu) \right]_{\mu=1+\nabla^2/2k^2} \rho(\mathbf{r}) \quad (10a)$$

and

$$V_{SO}(\mathbf{r}) = \frac{4\pi i\hbar^2(N-1)}{m} \times \left[\sum_l (c_l(k)/k^2) dP_l(\mu)/d\mu \right]_{\mu=1+\nabla^2/2k^2} \rho(\mathbf{r}), \quad (10b)$$

where

$$\int F(q) e^{i\mathbf{q} \cdot \mathbf{r}} d\mathbf{q} = (2\pi)^3 \rho(\mathbf{r}) \quad (11)$$

follows from (3). The high-energy optical potential obtained by combining (10) and (1) is energy-dependent and applies to the energy corresponding to the value of k appearing in (10) for which the expansion coefficients $a_l(k)$ and $c_l(k)$ are evaluated.¹³ In obtaining (10), it has been assumed that significant contributions to the integrals in (7) come only from values of q less than $2k$, this being the maximum value corresponding to the particular value of k for which the potential functions (10) are to be evaluated.¹⁴

The optical potential which follows from (1) and (10) is

$$V(\mathbf{r}) = \frac{-4\pi\hbar^2(N-1)}{m} \left\{ [a_0(k) + a_1(k)(1 + \nabla^2/2k^2) + a_2(k)(1 + 3\nabla^2/2k^2 + 3\nabla^4/8k^4) + \dots] \rho(\mathbf{r}) - \frac{i}{r} \frac{d}{dr} [c_1(k)/k^2 + (c_2(k)/k^2)(3 + 3\nabla^2/2k^2) + (c_3(k)/k^2)(6 + 15\nabla^2/2k^2 + 15\nabla^4/8k^4) + \dots] \rho(\mathbf{r}) \boldsymbol{\sigma} \cdot \mathbf{L} \right\}. \quad (12)$$

can be expressed in terms of Blatt-Biedenharn phase shifts with the help of Eq. (3.14) of reference 11. Blatt-Biedenharn nuclear phase shifts are given for four energies in Table I of reference 6.

¹⁴ In previous derivations of the high-energy optical potential (references 4, 5, and 6) the factors (8) have been evaluated at $\cos\theta = 1$ and then pulled out of the integrals in (7), the justifying argument being that, for a heavy target nucleus, $F(q)$ is a rapidly varying function of q peaked in the neighborhood of $q = 0$.

If the terms involving ∇^{2n} in (12) are neglected, the resulting optical potential has a central part which is proportional to the nucleon density in the target nucleus and a spin-orbit part which is proportional to the radial derivative of that density. This is the usual expression for the derived optical potential, obtained by replacing the factors (8) in the potential functions (7) by their values for $q=0$ ¹⁴:

$$V_{q=0}(\mathbf{r}) = \frac{-4\pi\hbar^2(N-1)}{m} \left\{ \bar{A}(k, q=0)\rho(r) - \frac{i}{r} [\bar{C}(k, q)(k^2 \sin\theta)^{-1}]_{q=0} \frac{d\rho(r)}{dr} \boldsymbol{\sigma} \cdot \mathbf{L} \right\}. \quad (13)$$

The ∇^{2n} terms in (12) contain the angle-dependence of the nucleon-nucleon scattering matrix [see Eqs. (10)]. When these terms are included, the radial dependence of the optical potential is no longer given by (13), but rather by

$$V(\mathbf{r}) = \frac{-4\pi\hbar^2(N-1)}{m} \times \left\{ \text{Re}\bar{A}(k, q=0)\rho'(k, r) + i \text{Im}\bar{A}(k, q=0)\rho''(k, r) - \frac{i}{r} \left(\text{Re}[\bar{C}(k, q)(k^2 \sin\theta)^{-1}]_{q=0} \frac{d\rho'''(k, r)}{dr} + i \text{Im}[\bar{C}(k, q)(k^2 \sin\theta)^{-1}]_{q=0} \frac{d\rho''''(k, r)}{dr} \right) \boldsymbol{\sigma} \cdot \mathbf{L} \right\}, \quad (14)$$

where the energy-dependent density functions $\rho^i(k, r)$ can be obtained from a comparison of (12) and (14). For example, $\rho'(k, r)$ is of the form

$$\rho'(k, r) = \sum_l \rho_l'(k, r) = [\text{Re}\bar{A}(k, q=0)]^{-1} \sum_l \text{Re}a_l(k) \times [1 + \sum_{n=1}^l d_{l,n} \nabla^{2n}/k^{2n}] \rho(r). \quad (15)$$

The effective density functions $\rho^i(k, r)$ are significantly different from the target nucleon density $\rho(r)$ in regions where the latter changes appreciably over a distance of the order of the de Broglie wavelength of the incident nucleon. Since the principal variation of the target nucleon density occurs at the nuclear surface,¹⁵ the ∇^{2n} terms in the optical potential (12) lead primarily to surface corrections to the usual derived optical potential (13).¹⁶

Evaluation of the expression (12) for the optical potential requires a knowledge of the nucleon-nucleon

singlet and triplet phase shifts and the nucleon density function $\rho(r)$. Summaries have been given by Moravcsik *et al.*¹⁷ of recent analyses of nucleon-nucleon scattering data, from which the phase shifts have been determined.¹⁸ The nuclear density function can be obtained from the nuclear charge distributions required to explain the electron-scattering data of Hofstadter *et al.*¹⁵ with the usual assumption that neutron and proton distributions are the same. For medium and heavy nuclei, a Fermi function seems to give an adequate representation of the nucleon density,¹⁵ but the detailed shape of this density has not been uniquely determined. What can be determined with some certainty by electron-scattering experiments are two shape parameters which Hofstadter takes to be the half-density radius c and the surface thickness t (distance in which the nucleon density falls from 90% to 10% of its central value). In experiments on gold, for example, the scattering data are consistent with the nucleon density functions

$$\rho(r) = \rho_F [e^{(r-c)/a} + 1]^{-1} \quad (\text{Fermi}) \quad (16a)$$

and

$$\rho(r) = \rho_{MG} [e^{(r^2-c^2)/b^2} + 1]^{-1} \quad (\text{modified Gaussian}) \quad (16b)$$

when they have values of c which differ by less than 0.5% and values of t which differ by about 10%.¹⁹

Although a knowledge of the detailed shape of the nucleon density $\rho(r)$ is required for an explicit evaluation of the optical potential (12), the two shape parameters, c and t , of $\rho(r)$ lead to a nearly shape-independent specification of the second and fourth moments of $\rho(r)$; and these moments uniquely determine the corresponding moments of the effective densities $\rho^i(k, r)$. The n th moment $\langle R^n \rangle'$ of the central-real effective density $\rho^i(k, r)$ is, for example, given by

$$\begin{aligned} \langle R^n \rangle' &= \int r^n \rho^i(k, r) dr / \int \rho^i(k, r) dr \\ &= \text{Re} \int r^n V_c(r) dr / \text{Re} \int V_c(r) dr. \end{aligned} \quad (17)$$

In particular, the second moment

$$\begin{aligned} \langle R^2 \rangle' &= -3 \left[\frac{1}{F(q)} \frac{d^2 F(q)}{dq^2} \right]_{q=0} \\ &\quad - 3 \left[\frac{1}{\text{Re}\bar{A}(k, q)} \frac{\partial^2 \text{Re}\bar{A}(k, q)}{\partial q^2} \right]_{q=0} \end{aligned} \quad (18)$$

has been given by Kerman *et al.*,^{6,20} and the fourth

¹⁵ See, for example, R. Hofstadter, Rev. Mod. Phys. 28, 214 (1956) and Ann. Rev. Nucl. Sci. 7, 231 (1957).

¹⁶ That this corresponds to taking account of the finite range of the nucleon-nucleon interaction is discussed following Eq. (19); see also references 6, 12, and 33.

¹⁷ M. H. MacGregor, M. J. Moravcsik, and H. P. Stapp, Ann. Rev. Nucl. Sci. 10, 291 (1960); M. J. Moravcsik and H. P. Noyes, *ibid.* 11, 95 (1961).

¹⁸ See also Table I of reference 6.

¹⁹ B. Hahn, D. G. Ravenhall, and R. Hofstadter, Phys. Rev. 101, 1131 (1956).

²⁰ Kerman, McManus, and Thaler suggested, in reference 6, the

moment is

$$\begin{aligned} \langle R^4 \rangle' = & 5 \left[\frac{1}{F(q)} \frac{d^4 F(q)}{dq^4} \right]_{q=0} + 5 \left[\frac{1}{\text{Re} \bar{A}(k, q)} \frac{\partial^4 \text{Re} \bar{A}(k, q)}{\partial q^4} \right]_{q=0} \\ & + 30 \left[\left(\frac{1}{F(q)} \frac{d^2 F(q)}{dq^2} \right) \right. \\ & \left. \times \left(\frac{1}{\text{Re} \bar{A}(k, q)} \frac{\partial^2 \text{Re} \bar{A}(k, q)}{\partial q^2} \right) \right]_{q=0}. \quad (19) \end{aligned}$$

The first terms in Eqs. (18) and (19) are the second and fourth moments of the nucleon density $\rho(r)$, respectively. The additional terms can easily be obtained from (8a) with the substitution $\mu = 1 - q^2/2k^2$ mentioned below Eqs. (8). The moments of the other effective densities can be obtained in a similar manner.

The terms in Eqs. (18) and (19) which involve $\bar{A}(k, q)$ take some account of the finite range of the nucleon-nucleon interaction. This can be seen most easily in Born approximation in which these terms are the second and fourth moments, respectively, of the central part of the nucleon-nucleon potential.

In the next section, evaluations of the effective density functions $\rho^i(k, r)$ are reported for assumed nucleon densities of the forms given in (16). The second and fourth moments of these effective densities have been used to specify the shape parameters c^i and l^i for effective density functions of assumed Fermi form.

III. RESULTS

The effective densities $\rho^i(k, r)$ in the optical potential (14) and their second and fourth moments have been evaluated for an incident nucleon energy of 310 MeV.²¹ These calculations are intended to illustrate the effects of the q dependence of the nucleon-nucleon scattering matrix on the high-energy optical potential rather than to provide an optical potential which can be used in the analysis of a particular scattering experiment. We have, therefore, omitted Coulomb effects²² (appropriate to the scattering of incident neutrons) and have neglected the neutron-excess terms in the average scattering matrix coefficients (6).²³ The calculations were made for assumed target nuclei which have a half-density radius $c = 6$ F, surface thicknesses $t = 2.42$

use of effective densities $\rho^i(k, r)$ which have the same shape as the nucleon density $\rho(r)$ but larger mean radii given by (18) and corresponding expressions for the other mean radii.

²¹ The procedure for calculating the expansion coefficients $a_l(k)$ and $c_l(k)$, from which the effective densities are determined by expressions such as (15), is given in footnote 13.

²² This means that, in the procedure outlined in footnote 13, the Coulomb phase shifts $\Phi_{j \pm 1}$ in Eq. (3.14) of reference 11 are set equal to zero, and the Blatt-Biedenharn phase shifts δ_l and $\delta_{l, j}$ are taken to be the Blatt-Biedenharn nuclear shifts given in Table I of reference 6.

²³ The magnitude of the contribution of the neutron-excess terms to the optical potential (13) is indicated in references 6 and 10.

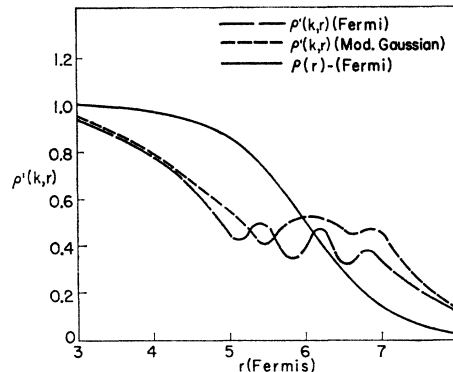


FIG. 1. Central-real effective densities $\rho^i(k, r)$ in units of ρ_F for target nuclei of Fermi and modified Gaussian shapes with shape parameters $c = 6$ F and $t = 2.42$ F.

and 2.86 F and nucleon densities of the Fermi and modified Gaussian forms given in (16).²⁴

The effective densities $\rho^i(k, r)$, $\rho^{ii}(k, r)$, and $\rho^{iii}(k, r)$ are displayed in Figs. 1–5, where they have been plotted in units of ρ_F , the central value of the Fermi function (16a). The effective densities are labeled according to the nucleon density $\rho(r)$ from which they follow (Fermi or modified Gaussian). The nucleon density function $\rho(r)$ of Fermi form (16a) is also shown on these figures in units of ρ_F ; the nucleon density function of modified Gaussian form is similar to the Fermi.^{25,26} Since $\rho(r)$ determines the radial dependence of the optical potential when the surface corrections are neglected [see Eq. (13)], comparisons of $\rho(r)$ and the effective densities $\rho^i(k, r)$ indicate the magnitude of these corrections.

Evaluation of the effective densities $\rho^i(k, r)$ requires the summing of infinite series of the form (15). The expansion coefficients $a_l(k)$ and $c_l(k)$, which appear in these sums and are defined in (8), decrease rapidly in magnitude with increasing l for values of l greater than the product of the range of the nucleon-nucleon interaction and the relative momentum k in the nucleon-nucleon center-of-mass system. The product of k and the pion Compton wavelength being 2.7 for the laboratory energy 310 MeV used here, the nuclear phase shifts used in these calculations were assumed to be zero for $l > 5$; consequently, the expansion coefficients $a_l(k)$ and $c_l(k)$ used here were also zero for $l > 5$. Use of the Blatt-Biedenharn nuclear phase shifts given by Kerman *et al.*^{6,22} for $l \leq 5$ led to adequate convergence for the sums corresponding to (15) for the effective densities $\rho^i(k, r)$ and $\rho^{iii}(k, r)$, shown in Figs. 2–5. For the

²⁴ These values of t are appropriate to medium and heavy nuclei, and the value of c is appropriate to a nucleus containing about 175 nucleons; see reference 15.

²⁵ See, for example, Fig. 5 of reference 19.

²⁶ For $c = 6$ F and $t = 2.42$ F, the coefficients in the nucleon densities (16) are related by $\rho_{MG} = 1.04\rho_F$. The effective densities $\rho^i(k, r)$ and $\rho^{ii}(k, r)$ corresponding to a nucleon density of modified Gaussian form, which are shown in Figs. 1 and 2, have central values 1.04 in units of ρ_F , whereas the effective densities corresponding to nucleon densities of Fermi form have the central value unity.

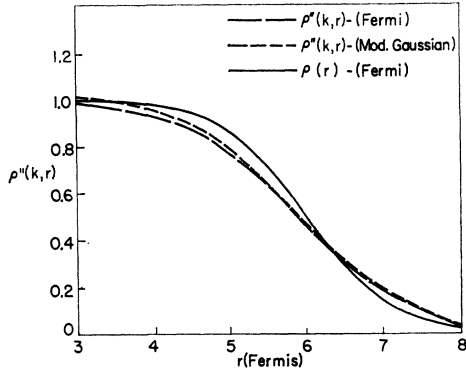


FIG. 2. Central-imaginary effective densities $\rho''(k,r)$ in units of ρ_F for target nuclei of Fermi and modified Gaussian shapes with shape parameters $c=6$ F and $t=2.42$ F.

effective density $\rho'(k,r)$, the convergence was marginal for $t=2.86$ F (see Fig. 4) and poor for $t=2.42$ F (see Fig. 1). The convergence for the effective density $\rho''(k,r)$ was not satisfactory with the phase shifts used here for either value of t . In fact, the second moment of $\rho''(k,r)$ was found to be smaller than that of the nucleon density $\rho(r)$ ²⁷; consequently, our results for $\rho''(k,r)$ are not reported here. The terms $\rho_l'(k,r)$ in the sum (15) for $\rho'(k,r)$ and those in the corresponding sum for $\rho''(k,r)$ are given in units of ρ_F in Figs. 6 and 7, respectively, for the surface thickness $t=2.42$ F; from these figures it appears that the neglect of the terms with $l>5$ is justified for $\rho''(k,r)$ but may not be for $\rho'(k,r)$.

The $l=5$ term $\rho_5'(k,r)$, shown in Fig. 6, gives a large oscillating contribution to $\rho'(k,r)$ in the neighborhood of the half-density radius c . These oscillations arise primarily from $\nabla^{10}\rho(r)/k^{10}$ and, to a lesser extent, from the lower powers of $\nabla^2\rho(r)/k^2$ in Eq. (15). The magnitudes of the $\nabla^{2n}\rho(r)/k^{2n}$ surface-correction terms in all the effective densities depend strongly upon the curvature of the nucleon density $\rho(r)$ and upon the energy of the incident nucleon. These terms are relatively

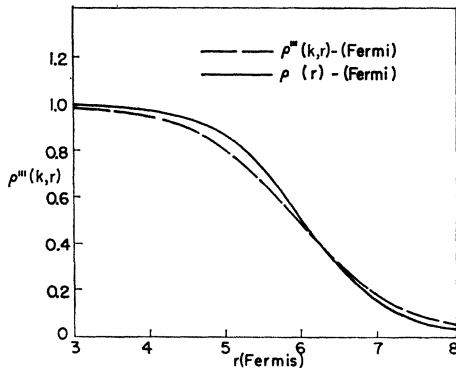


FIG. 3. Spin-orbit effective density $\rho'''(k,r)$ in units of ρ_F for a target nucleus of Fermi shape with shape parameters $c=6$ F and $t=2.42$ F.

²⁷ This inadequacy was indicated in reference 6.

more important for small energies than they are for large²⁸ and more important for nuclei with small surface thicknesses than they are for those with more diffuse surfaces.²⁹

The shape parameters c and t have been used to calculate the second moment $\langle R^2 \rangle$ and the fourth moment $\langle R^4 \rangle$ of a nucleon density $\rho(r)$ of assumed Fermi shape; these parameters and moments are given in the first four columns of Table I.³⁰ The corresponding

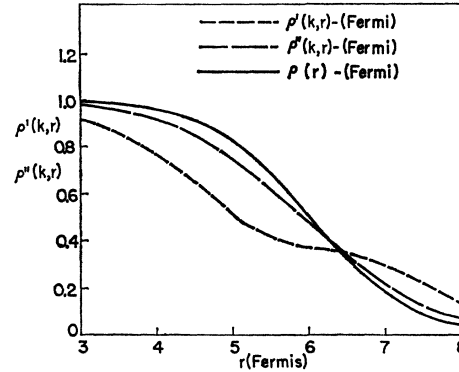


FIG. 4. Effective densities $\rho'(k,r)$ and $\rho''(k,r)$ in units of ρ_F for a target nucleus of Fermi shape with shape parameters $c=6$ F and $t=2.86$ F.

moments $\langle R^2 \rangle^i$ and $\langle R^4 \rangle^i$ of the effective densities $\rho^i(k,r)$, which were calculated in the manner indicated in Eqs. (18) and (19), are given in columns (5) and (6) of Table I. The values of the shape parameters c^i and t^i of Fermi functions, which have these second and fourth moments, are given in columns (7) and (8) of the table. Comparison of these parameters with those of the

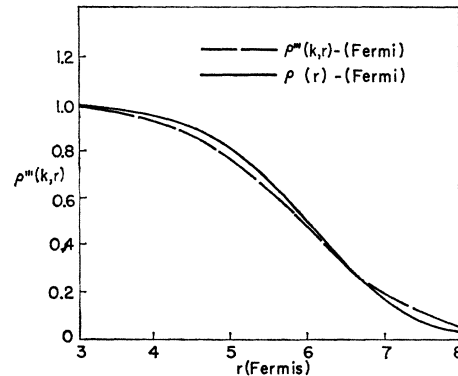


FIG. 5. Effective density $\rho'''(k,r)$ in units of ρ_F for a target nucleus of Fermi shape with shape parameters $c=6$ F and $t=2.86$ F.

²⁸ Calculations of $\rho'(k,r)$ and $\rho''(k,r)$ have also been made for an incident nucleon energy of 156 MeV. In this case, the convergence of the sums for the effective densities is not as good as that indicated in Figs. 6 and 7 in spite of the fact that the coefficients $a_l(k)$ decrease more rapidly with increasing l at 156 MeV than they do at 310 MeV.

²⁹ Compare the curves for $\rho'(k,r)$ shown in Figs. 1 and 4.

³⁰ The second and fourth moments of a nucleon density function of modified Gaussian form (16b), having the values $c=6$ F and $t=2.42$ F, are $\langle R^2 \rangle = 24.9$ F² and $\langle R^4 \rangle = 781$ F⁴.

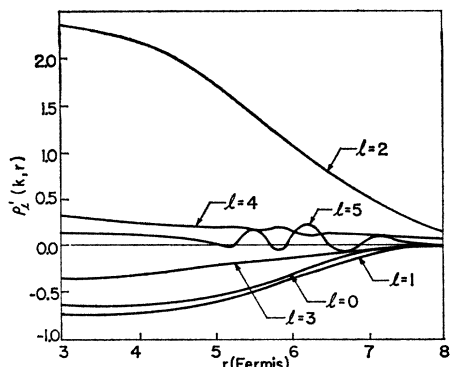


FIG. 6. Terms in the sum (15) for the effective density $\rho'(k, r)$ for a target nucleus of Fermi shape with shape parameters $c=6$ F and $t=2.42$ F.

nucleon density indicates the magnitude of the surface corrections discussed following Eq. (15).

The qualitative differences between the effective densities $\rho^i(k, r)$ and the nucleon density $\rho(r)$, which are indicated both in Figs. 1–5 and in Table I, are that the former have larger mean radii (and larger values of c in most cases) and more diffuse surfaces (larger values of t) than does the former.

TABLE I. Second and fourth moments and shape parameters of the effective densities $\rho^i(k, r)$, $\rho''(k, r)$, and $\rho'''(k, r)$ occurring in the optical potential (14).

Shape parameters and moments of nucleon density of Fermi form.				Moments and shape parameters of the effective densities of Fermi form.				
(1)	(2)	(3)	(4)	(5)	(6)	(7)	(8)	
c	t	$\langle R^2 \rangle$	$\langle R^4 \rangle$	$\langle R^2 \rangle^i$	$\langle R^4 \rangle^i$	c^i	t^i	
(F)	(F)	(F ²)	(F ⁴)	(F ²)	(F ⁴)	(F)	(F)	
6	2.42	25.9	871	$\rho'(k, r)$	33.5	1565	6.42	3.50
				$\rho''(k, r)$	27.6	1023	6.05	2.82
				$\rho'''(k, r)$	27.1	981	6.03	2.71
				$\rho'(k, r)$	35.0	1750	6.39	3.83
6	2.86	27.4	1018	$\rho''(k, r)$	29.1	1179	6.00	3.25
				$\rho'''(k, r)$	28.6	1134	5.98	3.17

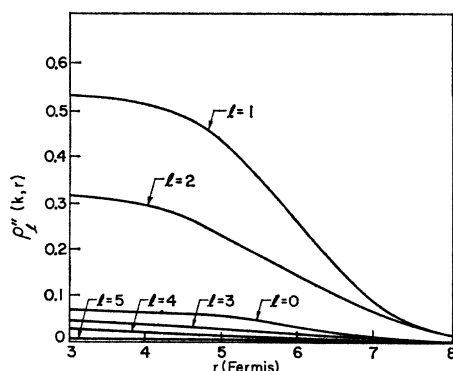


FIG. 7. Terms in the sum corresponding to (15) for the effective density $\rho''(k, r)$ for a target nucleus of Fermi shape with shape parameters $c=6$ F and $t=2.42$ F.

IV. CONCLUDING REMARKS

Phenomenological analyses of data from the scattering of high-energy nucleons by heavy nuclei have been made in terms of optical potentials of the form (1) with potential functions $V_c(r)$ and $V_{so}(r)$ whose radial dependence is of the same Fermi form (16a). These analyses have led to shape parameters c and t which are about 15% larger than the corresponding parameters of the appropriate nucleon density functions of Fermi form.^{2,31,32} The results of the present paper, given in Table I, indicate that the difference between these sets of parameters can be understood qualitatively in terms of surface corrections to the usual optical potential (13), which arise from the q dependence of the nucleon-nucleon scattering matrix. The calculations reported here led to radius parameters c^i which are slightly (0 to 5%) larger than that of the nucleon density $\rho(r)$ and to surface-thickness parameters t^i about 40% larger than that of $\rho(r)$ for the central-real effective density $\rho'(k, r)$ and about 15% larger for the central-imaginary effective density $\rho''(k, r)$ and for $\rho'''(k, r)$. The values of t^i obtained here for the central-imaginary effective density are in substantial agreement with the results of phenomenological analyses for incident nucleons of about 300 MeV. At these energies, the central-imaginary term in the optical potential is much larger than the central-real and will, therefore, dominate an analysis in which the same functional form is assumed for real and imaginary parts of the central potential.

The surface corrections to the optical potential lead to effective densities $\rho^i(k, r)$ which have not only different radii and surface thicknesses than does the nucleon density but also different functional forms, as can be seen in Eq. (12) and in Figs. 1–5.^{20,33}

An improved calculation of $\rho'(k, r)$ and even a qualitatively adequate calculation of $\rho''''(k, r)$ at 310 MeV will require the use of a more complete set of nucleon-nucleon phase shifts than those used here.³⁴ The reason for this was pointed out in Sec. III in connection with Figs. 1 and 6. It is, however, still a matter of conjecture whether the use of a complete set of phase shifts will lead to a smooth effective density $\rho^i(k, r)$ and to a satisfactory result for $\rho''''(k, r)$.

ACKNOWLEDGMENT

The authors are happy to acknowledge a helpful conversation with Professor H. McManus.

³¹ F. Bjorklund, I. Blandford, and S. Fernbach, Phys. Rev. **108**, 795 (1957).

³² A. E. Glassgold, Rev. Mod. Phys. **30**, 419 (1958).

³³ That the shapes of the effective densities are expected to be different from that of the nucleon density was pointed out by A. H. Cromer, Phys. Rev. **113**, 1607 (1959), R. Lipperheide and D. S. Saxon, *ibid.* **120**, 1458 (1960), and R. R. Johnson, Nucl. Phys. **36**, 368 (1962).

³⁴ See reference 17 for discussions of recent determinations of nucleon-nucleon phase shifts.